Mol. Cryst. Liq. Cryst., Vol. 520: pp. 97/[373]–107/[383], 2010

ISSN: 1542-1406 print/1563-5287 online
DOI: 10.1080/15421400903582857

Strong Ligand Field Effects of Blue Phosphorescent Iridium(III) Complexes

HO WAN HAM[1] AND YOUNG SIK KIM[1,2]

[1]Department of Information Display, Hongik University, Seoul, Korea
[2]Department of Science, Hongik University, Seoul, Korea

In this study, new deep blue emitting mixed ligand iridium(III) complexes such as $Ir(dFppy)(PPhMe_2)_2(H)(Cl)$, $[Ir(dFppy)(PPhMe_2)_2(H)(NCMe)]^+$ *and* $Ir(dFppy)(PPhMe_2)_2(H)(CN)$, *[dFppy = 2-(2′,4′-difluoro-phenyl)pyridine] were synthesized and studied to tune the phosphorescence wavelength to the deep blue region and to enhance the luminescence efficiencies. These iridium complexes comprise one cyclometalating, two phosphines trans to each other and two cis-ancillary ligands. We investigate the electron-withdrawing capabilities of ancillary ligands using the DFT and TD-DFT calculations on the ground and excited states of the three complexes to gain insight into the factors responsible for the emission color change and the different luminescence efficiency. Reducing the molecular weight of phosphine ligand with* $PPhMe_2$ *leads to a strategy of the efficient deep blue organic light-emitting devices (OLED) by thermal processing instead of the solution processing. The electron-withdrawing difluoro group substituted on the phenyl ring and the cyano strong field ancillary ligand in the trans-position to the carbon atom of phenyl ring increased HOMO-LUMO gap and achieved the hypsochromic shift in emission color. As a result, the maximum emission spectra of* $Ir(dFppy)(PPhMe_2)_2(H)(Cl)$, $[Ir(dFppy)(PPhMe_2)_2(H)(NCMe)]^+$ *and* $Ir(dFppy)(PPhMe_2)_2(H)(CN)$ *were in the ranges of 452, 443, 442 nm, respectively.*

Keywords Blue; iridium complex; mixed ancillary ligands; OLED materials; phosphorescence

1. Introduction

In the last few years, phosphorescent materials and devices have been extensively studied in order to achieve a high efficiency for organic light-emitting diodes (OLEDs) since Thompson et al. reported OLEDs with phosphorescent heavy metal complexes [1–3]. Heavy metals present in the complexes, such as iridium or platinum, are known to induce an intersystem crossing by strong spin-orbit coupling. This crossing leads to a mixing of the singlet and triplet excited states [4–8]. Radiative relaxation of the spin-forbidden nature from the triplet excited state is then allowed, resulting in high phosphorescence efficiencies. Thus, heavy metal complexes can serve as efficient phosphors in OLEDs. Unfortunately, most phosphorescent emitters have a long radiative lifetime, which leads to the dominant triplet-triplet

---

Address correspondence to Young Sik Kim, Department of Information Display, Hongik University, Seoul 121-791, Korea. E-mail: youngkim@wow.hongik.ac.kr

(T-T) annihilation at high currents. The occurrence of T-T annihilation diminishes the performance of phosphorescent material, particularly its maximum brightness and luminescence efficiency at high currents [9,10].

Until now, the development of a green and red emitter in fluorescent and phosphorescent displays has achieved in great success. However, pure blue-emitting complex dopants are not available. Hence, we have focused current research efforts on the syntheses of blue-emitting iridium complexes. Some phosphorescent blue-emitter materials have been synthesized and the results reported; particularly 2-phenylpyridine with added electro-withdrawing groups to the phenyl ring (fluoro, cyano group and others), and electro-donating groups added to the pyridyl ring (methyl group and others) exhibited good blue-emission characteristics [11,12].

In this study, new deep blue-emitting mixed-ligand iridium(III) complexes such as $Ir(dFppy)(PPhMe_2)_2(H)(Cl)$, $Ir(dFppy)(PPhMe_2)_2(H)(NCMe)^+$ and $Ir(dFppy)(PPhMe_2)_2(H)(CN)$, [dFppy = 2-(2′,4′-difluoro-phenyl)pyridine] were synthesized and studied to tune the phosphorescence wavelength to the deep blue region and to enhance its luminescence. These iridium complexes comprise of one cyclometalating and two phosphines trans to each other, and two cis-ancillary ligands. We investigated the strong field effects of ancillary ligands to gain insight into the factors responsible for the emission color change and the different luminescence efficiency. To analyze the color tuning by the effects of trans ligands to dFppy ligand on the luminescent property, we have measured the UV-absorption and photoluminescence (PL) spectra of iridium complexes, and have calculated these complexes theoretically by the density functional theory (DFT) Method.

2. Experimental Details

2.1. *Synthesis*

All ligands and reagents were purchased from Aldrich Co., except for Ir(III) trichloride hydrate ($IrCl_3 \cdot H_2O$), which was purchased from Strem Co. and used without further purification. All reactions were carried out under a nitrogen or argon atmosphere. Solvents were dried using standard procedures. All column chromatography was performed with the use of silica gel (230-Mesh, Merck). Iridium complex, $[Ir(COD)Cl]_2$ was synthesized by the literature methods.

2.1.1. *Synthesis of Ligand: dFppy.* dFppy was obtained from the reaction of 2-Chloropyridine with the corresponding 2,4-difluorophenyl-boronic acid by Suzuki coupling. 2-Chloropyridine (0.56 g, 5 mmol), 2,4-difluoro-phenylboronic acid (0.79 g, 5 mmol) and tetrakis-(triphenylphospine)palladium(0) (0.196 g, 0.17 mmol) were dissolved in 20 ml of toluene, 10 ml of ethanol and 20 ml of 2 N sodium carbonate aqueous solution. The mixture was refluxed at 110°C under the nitrogen atmosphere for eight hours. The mixture was cooled to room temperature and extracted with 20 ml of ethyl acetate. The organic fraction was dried over anhydrous $MgSO_4$, then filtered off and dried under vacuum. The residue was purified by silica gel chromatography using ethyl acetate/hexane (1:3). The product was collected and dried under vacuum.dfppy – Yield 60%, bright orange oil, MW: 192.2.

2.1.2. *Synthesis of Complex: $Ir(dFppy)(PPhMe_2)_2(H)(Cl)$.* Chloro(1,5-cyclooctadiene)iridium(I) dimmer $[Ir(COD)Cl]_2$ (0.2 g, 0.28 mmol), dimethylphenylphospine ($PPhMe_2$) (0.16 ml, 1.12 mmol) and dFppy (0.11 g, 0.56 mmol) were dissolved in 20 ml of 2-ethoxyethanol in a 50 ml flask. The mixture was refluxed at 90°C under the nitrogen atmosphere for six hours and then cooled to room temperature. The product portion was collected and washed with 20 ml of methanol, recrystallized in chloroform/n-pentane, and dried under vacuum.

Ir(dFppy)$(PPhMe_2)_2$(H)(Cl) – Yield 78%, pale-yellowish crystal.

2.1.3. *Synthesis of Complex: [Ir(dFppy)$(PPhMe_2)_2$(H)(NCMe)](OTf).* Ir(dFppy)$(PPh_2Me)_2$(H)(Cl) (0.082 g, 0.1 mmol), silver trifluoromethane sulfonate (AgOTf) (0.026 g, 0.1 mmol) and acetonitrile anhydrous (MeCN) (1 ml, 20 mmol) were dissolved in 10 ml of chloroform in a 50 ml flask. The mixture was stirred under the nitrogen atmosphere for two hours at normal temperature. After two hours of stirring, white powder of AgCl was removed by filtration and 20 mmol of MeCN was added once more into the product solution, and stirred under the nitrogen atmosphere for an extra two hours at normal temperature. 30 ml of n-pentane was added to yield pale-yellowish concentrated oil and residue were collected and washed with methanol and then dried under vacuum.

[Ir(dFppy)$(PPhMe_2)_2$(H)(NCMe)](OTf) – Yield 65%, yellowish concentrated oil.

2.1.4. *Synthesis of Complex: Ir(dFppy)$(PPhMe_2)_2$(H)(CN).* [Ir(dFppy)$(PPhMe_2)_2$(H)(NCMe)](OTf) (0.9 g, 0.1 mmol) and tetrabutylammonium cyanide (0.027 g, 0.1 mmol) were dissolved in 10 ml of methylene chloride in a 50 ml flask. The mixture was stirred under the nitrogen atmosphere for three hours at normal temperature. After six hours of stirring, 20 ml of n-pentane was added to yield pale-yellowish, concentrated oil. The residue was collected and washed with methanol and dried under vacuum.

Ir(dFMeppy)$(PPhMe_2)_2$(H)(CN) – Yield 63%, yellowish concentrated oil.

2.2. *Optical Measurements*

The UV-Vis absorption spectra were measured on Hewlett Packard 8425A spectrometer. The PL spectra were obtained on Perkin Elmer LS 55 spectrometer. UV-Vis and PL spectra of Ir(dFppy)$(PPhMe_2)_2$(H)(Cl), Ir(dFppy)$(PPhMe_2)_2$(H)$(NCMe)^+$ and Ir(dFppy)$(PPhMe_2)_2$(H)(CN) were measured in CH_2Cl_2 at room temperature.

2.3. *Theoretical Calculations*

Computationally, the electronic ground states of Ir(dFppy)$(PPhMe_2)_2$(H)(Cl), Ir(dFppy)-$(PPhMe_2)_2$(H)$(NCMe)^+$ and Ir(dFppy)$(PPhMe_2)_2$(H)(CN) were calculated using the B3LYP density functional theory (DFT). LANL2DZ [13] and 6-31G(d) [14] basis sets were employed for Ir and the other atoms, respectively. For the calculated ground state geometries, the electronic structures were examined in terms of the highest occupied molecular orbitals (HOMOs) and the lowest unoccupied molecular orbitals (LUMOs). Moreover, the electronic populations on the central atom were calculated to show the significant admixture of ligand π character with the amount of metal 5d character in the occupied molecular orbitals related to those metal-to-ligand charge-transfer (MLCT) transitions. To obtain the vertical excitation energies of the low-lying singlet and triplet excited states of the complexes, time-dependent density functional theory (TD-DFT) calculations using the B3LYP functional were performed at the respective ground-state geometry, where the basis set of ligands was changed to 6-31+G(d).

3. Results and Discussion

The colors of phosphorescent complexes used in OLEDs are tuned by the variation of both cyclometalating and ancillary ligands. Several small molecular and polymeric blue-emitting phosphorescent complexes have been reported, but the realization of highly efficient deep blue-emission remains a challenge. For the common 2-phenylpyridine (ppy) cyclometalating ligand, the highest occupied molecular orbital (HOMO) is localized on phenyl π and iridium 5d orbitals, while the lowest unoccupied molecular orbital (LUMO) is localized on the π^* orbitals of the pyridyl ring. To achieve deep blue-emission: (1) substituting fluoro groups on the 2′,4′-position of the phenyl ring of ppy ligand as electron withdrawing group to stabilize the HOMO and increase HOMO-LUMO gap, (2) changing ancillary ligands coordinated to iridium atom to phosphine and cyano groups. Both phosphine and cyano groups are known as very strong field ligands, and their inclusion in the coordination sphere can increase the HOMO-LUMO gap to achieve the hypsochromic shift in emission color, and (3) reducing the molecular weight of phosphine ligand for fabrication method by thermal processing instead of the solution processing.

The main ligands, dFppy, were prepared by the Suzuki coupling, as illustrated in Figure 1(a). The final iridium complex was obtained via several steps. In the first step, $[Ir(COD)Cl]_2$, $PPhMe_2$ and dFppy ligand were synthesized, as illustrated in Figure 1(b). In the second step, chlorine ligand of $Ir(F_2Meppy)(PPh_2Me)_2(H)(Cl)$ was replaced with MeCN ligand by precipitation reaction of Ag and Cl ions, as illustrated in Figure 1(c). Finally, in the third step, MeCN ligand was substituted with CN ligand, as illustrated in Figure 1(d). The overall reaction yields were approximately 60 to 78%, respectively.

The solution UV–Vis absorption of complexes has been measured, as shown in Figure 2. The interesting characteristics of the UV absorption spectra for $[Ir(dFppy)(PPhMe_2)_2(H)(NCMe)]^+$ resemble those of $Ir(dFppy)(PPhMe_2)_2(H)(CN)$. The highest energy absorptions are due to transitions centered on the dFppy ligands, and shoulder at ~270 nm is attributed to transitions centered on the phosphine ligand. Weaker levels at lower energy ($\lambda > 330$ nm) are due to spin-allowed singlet-to-singlet metal-to-ligand charge-transfer (^{1}MLCT) and spin-forbidden singlet-to-triplet ^{3}MLCT transitions. MLCT transition has been known for complexes containing heavy metal, such as iridium, in which spin-orbit coupling is strong [14,15]. It is slightly difficult to classify the ^{1}MLCT and ^{3}MLCT transitions in these compounds. However $[Ir(dFppy)\ (PPhMe_2)_2(H)(NCMe)^+$ and $Ir(dFppy)(PPhMe_2)_2(H)(CN)$ compounds display more blue shifted π-π^* and MLCT transition than that of the $Ir(dFppy)(PPhMe_2)_2(H)(Cl)$ compound. The ^{1}MLCT and ^{3}MLCT absorption peaks of $[Ir(dFppy)(PPhMe_2)_2(H)(NCMe)^+$ and $Ir(dFppy)(PPhMe_2)_2(H)(CN)$ are observed at 340~402 nm, whereas absorption peaks of $Ir(dFppy)(PPhMe_2)_2(H)(Cl)$ are observed at 357~411 nm. This was due to the strong field ancillary ligand, such as CN^-, lowering the HOMO energy level more than the weak field ancillary ligand, Cl^-. Ancillary ligands alter the MLCT energy, mainly by changing the HOMO energy level. The HOMO energy level may then be lowered by strong-field ancillary ligands, which causes a large d-orbital energy splitting. It is also

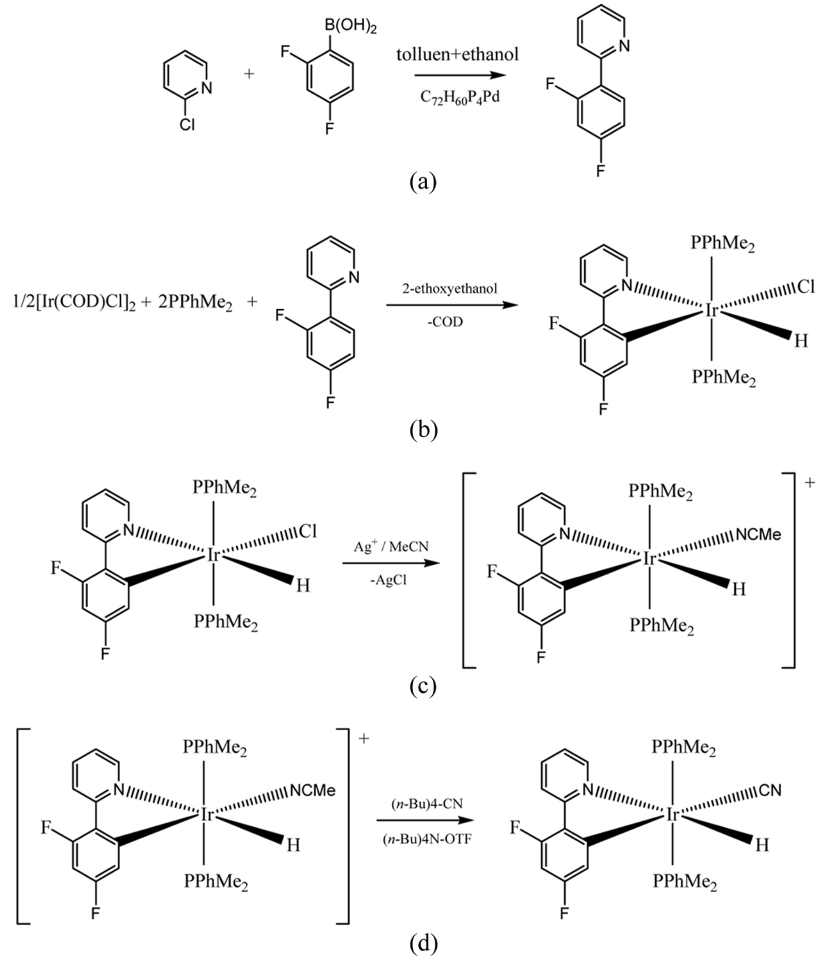

Figure 1. (a) Synthesis of dFppy ligand; (b) Synthesis of Ir(dFppy)$(PPhMe_2)_2$(H)(Cl); (c) Synthesis of $[Ir(dFppy)(PPhMe_2)_2(H)(NCMe)]^+$; (d) Synthesis of Ir(dFppy)$(PPhMe_2)_2$(H)(CN).

likely that strong field ancillary ligands lengthen the bond lengths of Ir–C (ppy) trans to the ancillary ligand to lower the energy levels of the dπ-orbitals of the metal, as strong field ligands are known to show a high trans effect. Medium filed ancillary ligand, MeCN, is located between them. Fluoro groups substituted on the 2′,4′-position of phenyl ring acted as the electron withdrawing group and increased the HOMO-LUMO energy gap and tune of the MLCT absorption peak to bluish. Figure 3 shows the calculated HOMO and LUMO energy levels and energy gap of iridium complexes on the optimized molecular structure of Ir(dFppy)$(PPhMe_2)_2$(H)(Cl) and Ir(dFppy) $(PPhMe_2)_2$(H)(CN) using DFT. The HOMO of Ir(dFppy)$(PPhMe_2)_2$(H)(CN) is stabilized compared to that of Ir(dFppy)$(PPhMe_2)_2$(H)(Cl) because of a high trans effect of the strong-field ancillary ligand, CN^-, which causes a significant blue shifted emission.

The PL spectra of iridium complexes in CH_2Cl_2 at room temperature are shown in Figure 4. The maximum emission spectra of Ir(dFppy)$(PPhMe_2)_2$(H)(Cl),

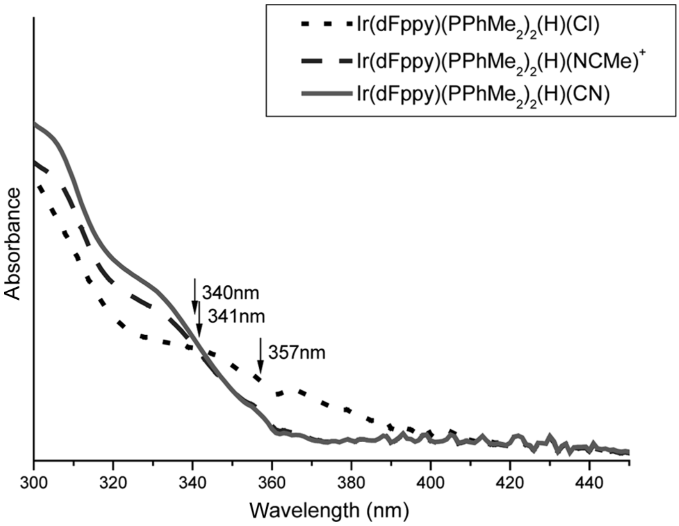

Figure 2. UV–Vis absorption spectra of Ir(dFppy)(PPhMe$_2$)$_2$(H)(Cl), [Ir(dFppy)(PPhMe$_2$)$_2$(H)(MeCN)]$^+$ and Ir(dFppy)(PPhMe$_2$)$_2$(H)(CN) in CH_2Cl_2 solution at room temperature.

[Ir(dFppy)(PPhMe$_2$)$_2$(H)(NCMe)]$^+$ and Ir(dFppy)(PPhMe$_2$)$_2$(H)(CN) were 452, 443, and 442 nm, respectively. The PL spectra of iridium complexes are compared with those of similar iridium complexes such as Ir(dFppy)(PPh$_3$)$_2$(H)(Cl), [Ir(dFppy)(PPh$_3$)$_2$(H)(NCMe)]$^+$ and Ir(dFppy)(PPh$_3$)$_2$(H)(CN) at 448, 441 and 441 nm, respectively [16]. Their PL spectra of Ir complexes are nicely matched with those of Ir complexes with PPhMe$_2$. Knowing that d-orbitals of iridium are involved in the HOMO of C^N complexes, such as Ir(C^N)$_3$ and Ir(C^N)$_2$LL′, one could expect the HOMO energy level to be lowered by strong field ligands more than by weak field ligands. A significantly longer wavelength emission band is measured for the

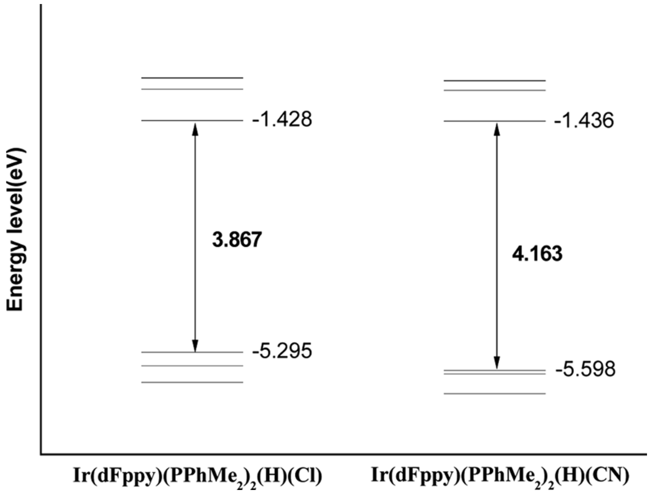

Figure 3. HOMO and LUMO energy levels of Ir(dFppy)(PPhMe$_2$)$_2$(H)(Cl), and Ir(dFppy)(PPhMe$_2$)$_2$-(H)(CN).

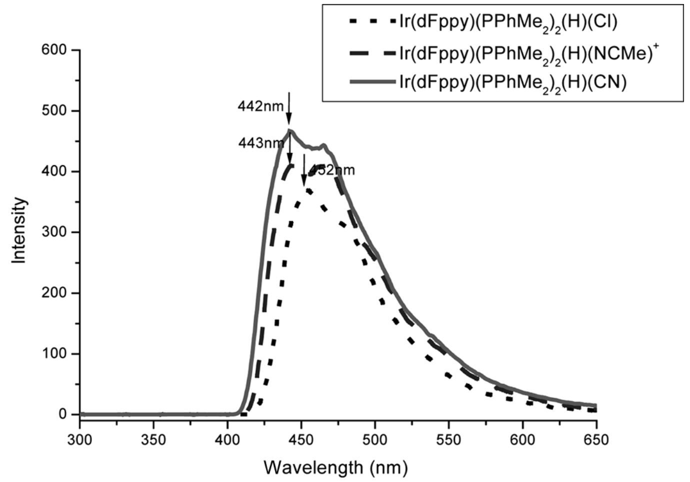

Figure 4. Relative PL emission spectrum of Ir(dFppy)(PPhMe$_2$)$_2$(H)(Cl), [Ir(dFppy)(PPhMe$_2$)$_2$(H)-(MeCN)]$^+$ and Ir(dFppy)(PPhMe$_2$)$_2$(H)(CN) in CH_2Cl_2 solution at room temperature.

complex that contains a chlorine ligand trans to the carbon of the C^N ligand, whereas the emission band is measured at much shorter wavelengths for all other complexes with a strong field ligand, such as CN^-. The trans and axial ligand PPhMe$_2$ is not involved in the HOMO of iridium complexes.

In order to examine which ligand mainly contributes to MLCT transition process of these complexes, the d-orbital characteristics of HOMOs and LUMOs were investigated after geometry optimization of the molecular structure of these complexes using DFT. Contour plots of the three highest HOMOs and three lowest LUMOs of Ir(dFppy)(PPhMe$_2$)$_2$(H)(CN) are shown in Figure 5. These orbitals

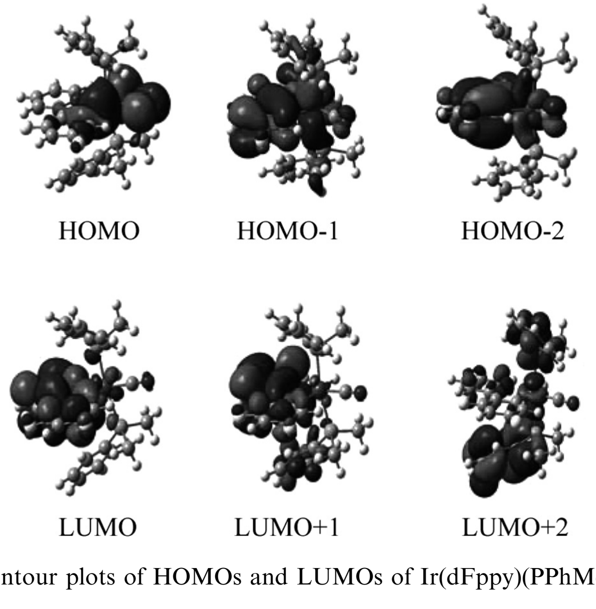

Figure 5. Contour plots of HOMOs and LUMOs of Ir(dFppy)(PPhMe$_2$)$_2$(H)(CN).

Table 1. Calculated excitation energies, dominant orbital excitation obtained and oscillator strengths obtained from TD-DFT calculations for Ir(dFppy)$(PPhMe_2)_2$(H)(Cl), [Ir(dFppy)$(PPhMe_2)_2$(H)-(MeCN)$]^+$ and Ir(dFppy)$(PPhMe_2)_2$(H)(CN)

	Singlets				Triplets		
Complex	Dominant excitation	Energy (eV)	Wavelength (nm)	Oscillator strengths	Dominant excitation	Energy (eV)	Wavelength (nm)
Ir(dFppy) $(PPhMe_2)_2$ (H)(Cl)	142 → 143	3.0828	402.17	0.0001	139 → 141	2.8717	431.74
	140 → 143	3.3621	368.77	0.0193	140 → 141	3.0234	410.08
	141 → 143	3.5711	347.18	0.0008	140 → 143	3.1138	398.17
	142 → 145	3.7019	334.92	0.0004	138 → 141	3.1937	388.22
	142 → 144	3.7675	329.09	0.0400	137 → 141	3.4541	358.94
	139 → 143	3.7893	327.19	0.0009	139 → 142	3.5128	352.94
	140 → 145	3.8852	319.12	0.0101	139 → 143	3.5304	351.18
	139 → 143	3.9407	314.62	0.0159	135 → 143	3.6329	341.28
	141 → 144	4.0352	307.25	0.0629	140 → 142	3.6494	339.74
	140 → 144	4.0917	303.01	0.0394	132 → 145	3.6728	337.58
Ir(dFppy) $(PPhMe_2)_2$ $(H)(NCMe)^+$	142 → 143	3.6738	337.48	0.0469	141 → 143	2.9438	421.17
	140 → 143	3.9033	317.64	0.0001	142 → 143	3.4552	358.83
	141 → 143	4.0388	306.98	0.1009	142 → 144	3.6004	344.36
	142 → 145	4.2737	290.11	0.0359	138 → 148	3.6546	339.25
	142 → 144	4.3284	286.44	0.0191	139 → 146	3.6740	337.47

	139 → 143	4.3878	282.56	0.0039	140 → 143	3.8036	325.96
	140 → 145	4.4931	275.94	0.0005	141 → 144	3.9340	315.16
	139 → 143	4.5146	274.63	0.0055	142 → 145	4.0103	309.16
	141 → 144	4.5903	270.10	0.0145	142 → 152	4.1773	296.80
	140 → 144	4.6225	268.22	0.0002	140 → 145	4.1938	295.63
Ir(dFppy)$(PPhMe_2)_2$(H)(CN)	138 → 139	3.3934	365.37	0.0002	137 → 139	2.9410	421.57
	137 → 139	3.5310	351.13	0.0386	137 → 139	3.3042	375.23
	136 → 139	3.9788	311.61	0.0571	138 → 139	3.3331	371.98
	138 → 140	3.9820	311.36	0.0025	137 → 140	3.5399	350.25
	134 → 139	4.0298	307.67	0.0001	132 → 144	3.6370	340.89
	137 → 140	4.0475	306.32	0.0062	133 → 143	3.6704	337.79
	138 → 141	4.0888	303.22	0.0021	135 → 139	3.7255	332.79
	135 → 139	4.1785	296.72	0.0673	138 → 140	3.9114	316.98
	137 → 141	4.2101	294.49	0.0429	138 → 141	3.9254	315.85
	133 → 139	4.4056	281.42	0.0009	138 → 140	4.0271	307.87

Table 2. Comparison of calculated bond lengths of Ir-C, Ir-N, and Ir-ancillary(A) for Ir(dFppy)-$(PPhMe_2)_2$(H)(Cl), [Ir(dFppy)$(PPhMe_2)_2$(H)(NCMe)$]^+$, and Ir(dFppy)$(PPhMe_2)_2$(H)(CN)

Complex	Ir-C (Å)	Ir-N (Å)	Ir-A (Å)
Ir(dFppy)$(PPhMe_2)_2$(H)(Cl)	2.098	2.060	2.470
Ir(dFppy)$(PPhMe_2)_2$(H)(NCMe)$^+$	2.106	2.074	2.000
Ir(dFppy)$(PPhMe_2)_2$(H)(CN)	2.103	2.133	1.980

are important because dominant excitations and emissions mainly occur by the electronic transition among these orbitals. In the HOMO side, most of the electron population of Ir(dFppy)$(PPhMe_2)_2$(H)(CN) is localized at iridium atom and the ancillary ligand CN^-. This effect can destabilize the MLCT state, leading to the luminescence wavelength in the blue region.

TD-DFT calculations were employed to examine the low-lying singlet and triplet states of Ir(dFppy)$(PPhMe_2)_2$(H)(Cl), [Ir(dFppy)$(PPhMe_2)_2$(H)(NCMe)$]^+$ and Ir(dFppy)$(PPhMe_2)_2$(H) (CN). Calculated excitation energies, dominant orbital excitation obtained, and oscillator strengths are shown in Table 1. The excitation energy of Ir(dFppy)$(PPhMe_2)_2$(H)(Cl), [Ir(dFppy)$(PPhMe_2)_2$(H)(NCMe)$]^+$ became greater than that of Ir(dFppy)$(PPhMe_2)_2$(H)(Cl), with a difference of 0.069~0.072 eV, which is a hypsochromic shift of about 10 nm in wavelength. Strong field ancillary ligands alter the MLCT energy mainly by changing the HOMO energy level. The HOMO energy level may then be lowered by strong-field ancillary ligands, which causes significant d-orbital energy splitting. It is also likely that strong-field ancillary ligands lengthen the bond lengths of Ir–C (ppy) trans to the ancillary ligand, which lowers the energy levels of the dπ-orbitals of the metal. Comparison of calculated bond lengths for Ir(dFppy)$(PPhMe_2)_2$(H)(Cl), [Ir(dFppy)$(PPhMe_2)_2$(H)(NCMe)$]^+$ and Ir(dFppy)$(PPhMe_2)_2$-(H)(CN) are summarized in Table 2. Therefore, it can be said that the ancillary ligand of CN induced the blue shift.

As a result, the PL spectrum of Ir(dFppy)$(PPhMe_2)_2$(H)(CN) shows a significant blue shifted phosphorescence emission, due to the substitution of fluoro groups in the phenyl ring. The fluoro groups in the phenyl ring pulls the HOMO level of iridium complexes and the strong field ancillary such as CN^-, which helps enlarge HOMO-LUMO energy gap to achieve the hypsochromic shift in emission color.

4. Conclusions

We have synthesized and studied photophysical properties of phosphorescent mono-cyclometalated iridium (III) complexes, having one cyclometalating and two phosphines trans to each other and two cis-ancillary ligands, such as Ir(dFppy) $(PPhMe_2)_2$(H)(Cl), Ir(dFppy)$(PPhMe_2)_2$(H)(NCMe)$^+$ and Ir(dFppy)$(PPhMe_2)_2$(H) (CN). The purpose was to find an efficient blue-emitting material for the OLED with thermal processing by tuning the ancillary ligand and reducing the molecular weight of phosphine ligands. We also investigated the electron-withdrawing capabilities of ancillary ligands using the DFT and TD-DFT calculations on the ground and excited states of the three complexes to gain insight into the factors responsible for the emission color change and the different luminescence efficiency.

The PL spectra of Ir(dFppy)($PPhMe_2$)$_2$(H)(CN) shows strong field effects of ancillary ligands, leading to a significant blue shifted phosphorescence, as well as higher luminescence efficiency due to replacing chlorine with the CN ligand. This study shows that the new type of mixed iridium complex, Ir(dFppy)($PPhMe_2$)$_2$(H)(CN) could act as a good radiation characteristic blue dopant for the fabrication of thermal processing in new phosphorescent OLEDs.

Acknowledgment

This work was supported by Hongik University Sabbatical Research Funds.

References

[1] Baldo, M. A., Thompson, M. E., & Forrest, S. R. (2000). *Nature*, *403*, 750.

[2] Baldo, M. A., Lamansky, S., Burrows, P. E., Tompson, M. E., & Forrest, S. R. (1999). *Appl. Phys. Lett.*, *75*, 4.

[3] Park, Y. H. & Kim, Y. S. (2007). *Thin Solid Films*, *515*, 5084.

[4] Baldo, M. A., Thompson, M. E., & Forrest, S. R. (1999). *Pure Appl. Chem.*, *71*, 2095.

[5] Brooks, J., Babaya, T., Lamansky, S., Djurovich, P. I., Tsyba, I., Bau, R., & Thompson, M. E. (2002). *Inorg. Chem.*, *41*, 3055.

[6] Kohler, A., Wilson, J. S., & Friend, R. H. (2002). *Adv. Mater.*, *14*, 701.

[7] Tamayo, A. B., Alleyne, B. D., Djurovich, P. I., Lamansky, S., Tsyba, I., Ho, N. N., Bau, R., & Thompson, M. E. (2003). *J. Am. Chem. Soc.*, *125*, 7377.

[8] Dedeian, K., Shi, J., Shepherd, N., Forsythe, E., & Morton, D. C. (2005). *Inorg. Chem.*, *44*, 4445.

[9] Kohler, A., Wilson, J. S., & Friend, R. H. (2002). *Adv. Mater.*, *14*, 701.

[10] Dedeian, K., Shi, J., Shepherd, N., Forsythe, E., & Morton, D. C. (2005). *Inorg. Chem.*, *44*, 4445.

[11] Park, N. G., Choi, G. C., Lee, Y. H., & Kim, Y. S. (2006). *Curr. Appl. Phys.*, *6*, 620.

[12] Takizawa, S., Nishida, J., Tsuzuki, T., Tokito, S., & Yamashita, Y. (2007). *Inorg. Chem.*, *46*, 4308.

[13] Hay, P. J. & Wadt, W. R. (1985). *J. Chem. Phys.*, *82*, 270.

[14] Hehre, W. J., Ditchfield, R., & People, J. A. (1972). *J. Chem. Phys.*, *56*, 2257.

[15] Seo, J. H., Kim, I. J., Kim, Y. K., & Kim, Y. S. (2008). *Jpn. J. Appl. Phys.*, *47*, 6987.

[16] Eum, M., Chin, C. S., Kim, S. y., Kim, C., Kang, S. K., Hur, N. H., Seo, J. H., Kim, G. Y., & Kim, Y. K. (2008). *Inorg. Chem.*, *47*, 6289.